3D Simulation and Optimization of Characteristics of $Al_{0.1}Ga_{0.9}N/In_{0.2}Ga_{0.8}N$ High Electron Mobility Transistor with $B_{0.03}Ga_{0.97}N$ Back-Barrier Layer

Fatima Zahra Bechlaghem (bechlaghem_f@yahoo.fr)
Universite Abou Bekr Belkaid Tlemcen Faculte des Sciences https://orcid.org/0000-0002-3393-7233
Abedelkader Hamdoune
Universite Abou Bekr Belkaid Tlemcen

Research Article

Keywords: HEMT, AlGaN/InGaN, BGaN, Back-barrier, AC and DC performance.

Posted Date: May 20th, 2021

DOI: https://doi.org/10.21203/rs.3.rs-370364/v1

Abstract

The objective of this paper is to simulate the effect of a BGaN back-barrier on performances of a high electron mobility transistor (HEMT) based on AlGaN/InGaN, by using TCAD 3D Silvaco simulator. We simulate some DC and AC characteristics; we note that with only 60 nm BGaN back-barrier layer and 3% of boron in BGaN, HEMT shows improvement of 33.34% in the maximum drain current, 64.7 % in the transconductance, 19% in the threshold voltage, 50% the drain-induced barrier lowering, 34.67% in the subthreshold swing, 20% in the breakdown voltage, 10.18% in the cut-off frequency, 12% in the maximum oscillation frequency, and record high ION/IOFF of over $10^{12.9}$.

Introduction

The synthesis The development of civil and military communication systems, such as radar or mobile telecommunications, requires electronic components capable of generating high power levels in the microwave domain[1] New technologies are being explored to meet these two operating criteria. The high electron mobility field effect transistor (HEMT), combined with wide band gap semiconductors such as Gallium Nitride, appears to be an excellent candidate for this type of application.[2] In fact, this HEMT based on AlGaN/InGaN heterostructure has both a high density of carriers confined to the heterojunction and high electronic mobilities. Cut-off frequencies up to several tens of gigahertz are also obtained.

Exploring new materials and their properties is one of the most important things to expand the range of applications. In most cases, this translates into new band gap gaps or network parameters that dictate the mechanical, electrical, or optical behavior of a device.[3] It allows for band engineering and to obtain a new wavelength or new electrical properties. Among the nitride-based semiconductors that have a wide band gap, a new class of materials has emerged based on the boron alloy, electrochemical films, BGaN alloy is a new material that has not been studied very much until now. Recently, a Japanese team has shown the possibility of developing the BGaN ternary by incorporating a small molar fraction of boron into GaN (up to 1% boron) [4] Beyond this small percentage, the fundamental difficulty is to avoid phase separation GaN-BN in which the alloy is no longer formed, rich zones in boron or rich in gallium appear in the layer.

Our work fits into this context; it consists in simulating the electrical performances of a AlGaN/InGaN HEMT which contains a boron gallium nitride (BGaN) back-barrier layer under the (InGaN) channel layer and comparing them to those of the transistor without this back-barrier layer.

Proposed structure and simulation model

The ideal Several works exist on the AlGaN/InGaN HEMT structures but very little on the AlGaN/InGaN/BGaN HEMT. The purpose of our work is therefore to make a comparison between these two structures, we use Silvaco software under the module DevEdit 3D and Atlas to obtain different characteristics.

The structures of the proposed AlGaN/InGaN HEMTs without and with BGaN back-barrier layer are shown in Fig. 1. (a) and (b). We consider H4-SiC substrate, 69 nm of undoped GaN buffer layer, 10 nm of undoped $In_{0.2}Ga_{0.8}N$ channel layer, 1 nm of undoped $In_{0.2}Ga_{0.8}N$ spacer layer, 8 nm of $Al_{0.1}Ga_{0.9}N$ delta layer with a donors doping density of $3\times10^{18}cm^{-3}$, 5 nm of undoped $Al_{0.1}Ga_{0.9}N$ Schottky layer, 5 nm GaN of cap layer (source), and 13 nm of GaN cap layer (drain) with donor doping density of $5\times10^{18}cm^{-3}$. Drain and Source ohmic contacts were performed by alloying evaporated gold metal[5] , and deposited on GaN cap layer. In (b)-HEMT, we add 60 nm of $B_{0.03}Ga_{0.97}N$ back barrier layer under the channel. The starting point for our simulations is a basic structure shown in Fig. 1. (b). The structure dimensions are 1.0 × 1.0 × 1.0 × 10^3 nm3.

As shown in fig Fig. 1.(c); the source has hollow square shape, the drain has rectangle shape, and the gate is placed on non-heavily doped semiconductor to generate the Schottky contact by using gold which has a work function of 4.55 V.

An empirical new model, relating walkout parameters and device structure, has been developed the key geometrical layout parameters with the gate dimensions of 600 × 50.0 × 600 nm^{-3}.

Semiconductor device physics consists of setting equations densities such as Poisson's equation and continuity equation for both electrons and holes under steady-state conditions.[6,7]

The simulation was performed in 3D with GUMMEL-NEWTON as the numerical method to resolve Poisson and continuity equations.

The Poisson equation makes it possible to establish a relationship between the variations of the electrostatic potential and the density of the electric charge.

$$div(\varepsilon\nabla\emptyset) = -p$$

where ε is the electrostatic potential, ψ is the local permittivity, and ρ is the local space charge density.

The continuity equations describe the temporal variations of the charge densities (electrons, holes); they are defined by the Eq (2) and (3).

where n and p are the electron and hole concentrations, Jn and Jp
are the electron and hole current densities, Gn and Gp are the generation rates for electrons and holes, Rn and Rp are the recombination rates for electrons rates for electrons and holes, and q
is the magnitude of the charge on an electron.

The basic band parameters for defining heterojunctions in Blaze are bandgap parameter, electron affinity, permittivity, and mobility.

The Energy band gap of the $B_xGa_{1-x}N$ depending on the boron fraction can be approximated using a modified Vegard's law including the bowing parameter (b)[8,9], in addition to the linear interpolation; this is

given by Eq. (4).

$$E_g(B_xGa_{1-x}N) = xE_g(BN) + (1-x)E_g(GaN) - bx(1-x) \quad (4)$$

$$E_g(B_xGa_{1-x}N) = 5.5x + (1-x)3.4 - 9x(1-x) \quad (5)$$

We consider $E_g(BN) = 5.5$ eV,

$E_g(GaN) = 3.4$ eV, b=9 eV at300K.[10,11,12,13]

Table 1. The relevant material for ($B_xGa_{1-x}N$) at x=0.03 parameters used in this simulation.

Parameter	Symbol	Value
Electron affinity (eV)	χ	4.1
Permittivity (F/m)		9.7
The electron mobility (cm^2/Vs)	μe	30
The hole mobility	μh	20

Results And Discussions

Generally, accurate simulation saves expensive technological efforts to obtain remarkable improvements of device characteristics.[14] The AlGaN/InGaN HEMT with and without BGaN Back-barrier layer was simulated using Silvaco ATLAS simulator.

The drain current (Id) versus drain voltage (Vd) (output characteristic) for (a)-HEMTs and (b)-HEMTs.

At Vg = − 3.0 V, − 2.5 V, − 2.0 V, − 1.5 V, − 1.0 V, − 0.5 V and 0.0 V are shown in Fig. 1a and b respectively.

At Vds = 10 V and Vg = 0 V; we obtain a maximum drain current of 6200 μA/mm and 9300 μA/mm, respectively for (a)-HEMTs and (b)-HEMTs.

The use of a BGaN back-barrier layer, the resistivity of the buffer layer under the channel increases and creates an electrostatic barrier, which prevents electron leakage from the channel to the substrate; then the drain current increases.[15]

The transfer characteristic is shown in Fig. 3. we obtain a threshold voltage (Vth) of about −4.25 V and − 3.5 V, respectively for HEMT with and without BGaN back-barrier layer.

Fig. 4. Shows the transconductance (Gm) as a function of the gate-source voltage (Vgs), with a fixed drain-source voltage (Vds) equal to 10 V, at room temperature. The maximum extrinsic transconductance is 3168.8 μS/mm and 9002.3μS/mm, respectively without and with boron.

Fig. 5 shows the evolution of the logarithmic plot of the drain-source current (Ids) versus to the gate-source voltage (Vgs), with a fixed drain-source voltage (Vds) equal to 10 V, at the room temperature. We

use the logarithmic plot to calculate the Ion/Ioff ratio. For the (b)-HEMT with the back-barrier, the Ion = $10^{-2.0}$ A and Ioff = $10^{-14.9}$ A resulting in an Ion/Ioff ratio of $10^{12.9}$.

The incorporation of boron in GaN increases the resistivity of the BGaN back-barrier layer and improves the mobility of the carriers in the active layer; this layer makes the buffer layer more resistant so that the leakage of electrons from the channel to the substrate becomes more difficult, it serves as an electrostatic barrier.

Where we notice that without the back-barrier (a)-HEMT, the Ion = $10^{-2.2}$ A and the Ioff =$10^{-7.8}$ A resulting in an Ion/Ioff ratio of $10^{5.5}$, so the (b)-HEMT exhibit an Ion/Ioff ratio better than the (a)-HEMT because of the BGaN Back-barrier.We get an Ion / Ioff ratio that is almost $10^{7.4}$ times larger for (a)-HEMT.

The sub-threshold swing (SS) is determined on the log (Ids) characteristic as a function of Vgs. It corresponds to the gate-source voltage to be applied to reduce the drain current by one decade. It is obtained for Vgs values close to the pinch, and is defined in mV/dec (variation of Vgs when Ids is divided by ten).

Fig. 6a and b Shows the transfer characteristics: the drain-source current (Ids) as a function of gate source voltage (Vgs) while the drain voltage was fixed at 2.0 V and 15.0 V, and the gate-source voltage was swept from 0.0 V to -10.0 V.

The Drain Induced Barrier Lowering (DIBL) is an important parameter describing electrostatic integrity of the High Electron Mobility Transistor (HEMT).

We calculate the Vth threshold voltage for two different values of Vds: 2.0 V and 15.0 V For without boron ; Vth = - 3.6 V and Vth = -3.8 V and with boron Vth = - 4.4 V and Vth = -4.8 V , respectively. Abs [ΔVth / ΔVds] ratio corresponds to the DIBL. We obtain a DIBL of 15 mV/V, 30 mV/V without and with boron respectively .

$SS_{\text{with boron}}$= ΔVgs/Δlog(Ids) = ΔVgs/dec = [-4.6+4.75]

V/dec = 0.150 V/dec = 150 mV/dec.

$SS_{\text{without boron}}$ = ΔVgs/Δlog(Ids) = ΔVgs/dec = [-3.5+3.6]

V/dec= 0.10 V/dec = 100 mV/dec.

Fig. 7a and b. Shows the gate-leakage current as a function of gate-source voltage, while the drain bias is fixed at Vds=10.0 V and the gate source is swept from Vgs 0.0 V to - 10.0 V without and with BGaN .

For (a) HEMT device based on nitride materials. The gate-leakage current is invariant with the gate bias, the device offers a gate leakage only of 9.10^{-7} A at 0.2 V gate bias.

For the (b)-HEMT with the back-barrier, the gate-leakage current is invariant with the gate bias, the device offers a gate leakage only of 7.10^{-35} A at -0.2 V, where we notice that with the back-barrier (b)-HEMT, the gate leakage only of 7.10^{-35}A. This extremely low value is evident to indicate the high quality of the device

The frequency device performance is studied by small-signal AC analysis, the cut-off frequency (f_t) and the maximum oscillation frequency (f_{max}). We study the influents of a BGaN back-barrier on characteristics RF of an high electron mobility transistor (HEMT). Fig. 8a and b shows two important parameters in high frequency which are the cut-off frequency (f_t) for which the modulus of the current gain is equal to 1 (0dB) and the maximum oscillation frequency (f_{max}) for which the modulus of the current gain is equal to 1 (0dB), at Vgs = 0 V and Vds = 10V. the $(f_t)_{without\ Boron}$ of 102.25 GHz , the $(f_{max})_{without\ Boron}$ of 878.5 GHz and the $(f_t)_{with\ Boron}$ of 117.5 GHz , the $(f_{max})_{with\ Boron}$ of 995.2 GHz respectively.

When the boron added , the BGaN ternary compound becomes more resistive and opposes better the leakage of the charge carriers towards the substrate.

Table.2 The most important results found are summarized.

Device's characteristics of HEMT	HEMT AlGaN/InGaN	HEMT AlGaN/InGaN/$B_{0.03}Ga_{0.97}N$
Drain current Ids (µA/mm)	6200	9300
Threshold voltage Vth (V)	-3.5	-4.25
Transconductance gm (µS/mm)	3168.8	9002.3
Drain Induced Barrier Lowring DIBL (mV/V)	15	30
Sub-threshold Swing SS (mV/dec)	100	150
Gate-leakage current (A)	9.10^{-7}	7.10^{-35}
Ion/Ioff ratio	$10^{5.5}$	$10^{12.9}$
Cut-off frequency f_t (GHz)	102.25	117.5
Maximum oscillation frequency f_{max}(GHz)	878.5	995.2

Conclusion

The In this article we presented the static and dynamic results obtained by AlGaN/InGaN HEMT on H4-SiC substrate transistor simulation with and without $B_{0.03}Ga_{0.97}N$ back- barrier layer analysis have been performed using 3D SILVACO-TCAD software.

The DC and AC properties were compared and investigated, our results allow us to conclude that device performance continuously augment with of $B_{0.03}Ga_{0.97}N$ back- barrier layer. It is found that the saturation drain current , the peak transconductance , SS, DIBL, the cut-off frequency (ft), the maximum oscillation frequency (fmax) and rapport ION/IOFF increases identically with $B_{0.03}Ga_{0.97}N$ back- barrier layer.

It can be said that a layer of BGaN can be very resistive with only a few percent boron, which could be very interesting for devices such as HEMTs, the proposed device structure is promising for high-performance and high-speed applications.

Declarations

CONFLICT OF INTEREST

The authors declare that they have no conflict of interest.

References

1. C. Chiu, S.C Yang, F.T Chien, Y.J Chan. Improved device linearity of AlGaAs/ InGaAs HFETs by a second mesa etching. *IEEE Electron Dev* Lett 2002;23:1–3.
2. Joshin, T. Kikkawa, H. Hayashi, S. Yokogawa, M. Yokoyama, N. Adachi, and M. Takikawa, “A 174 W high-efficiency GaN HEMT power amplifier for W-CDMA base station applications,” *in IEDM Tech*. Dig., Dec. 2003, pp. 983–985.
3. Morkoç, Handbook of Nitride Semiconductors and Devices, vols. I-III, Wiley-VCH, Berlin, 2008.
4. Kurimoto, T. Takano, J. Yamamoto, Y. Ishihara, M.Hoie, M. Tsubamoto, and H. Kawanishi Growth of BGaN/AlGaN multi-quantum-well structure by metalorganic vapor phase epitaxy J. Cryst. Growth 221, 378 (2000).
5. Ahmad,student of SEECS have submitted the final draft copy of his/her thesis titled: “ Physical device modeling and simulations of phemts, Reg. No.2010-*Nust-Ms*-EE(S)-48.
6. S. Yuan and J.J. Liou. Semiconductor device physics and simulation. Singerpr Science & Business Media, 2013. 46, 47, 48.
7. Piprek. Semiconductor *Optoelectronic Devices* : Introduction to Physics and Simulation. Academic Press, October 2013. Google-Books-ID : qqVuFz1kDp0C. 23, 46, 47, 48.
8. Orsal, Y. El Gmili, N. Fressengeas, J. Streque, R. Djerboub, T. Moudakir, S. Sundaram, A. Ougazzaden, and J.P. *Salvestrini, Optical Society of America OCIS codes*: (310.6860) (2014).
9. Piprek, Semiconductor Optoelectronic Devices: Introduction to Physics and Simulation. UCSB: Academic Press (2003): 22.
10. Dingle, D.D. Sell, S.E. Stokowski, M. Ilegems*, Phys. Rev*, B 41211, (1971).
11. L. Rumyantsev, M. E. Levinshtein, A. D. Jackson, S. N. Mohammmad,G. L. Harris, M. G. Spencer, and M. S. Shur;in Properties of Advanced Semiconductor Materials GaN, AlN, InN, BN, SiC, SiGe, edited by

M.E.Levinshtein, S. L. Rumyantsev, and M. S. Shur ,Wiley, *New York*,(2001), pp. 67–92.

12. Bougrov, M. E. Levinshtein, S. L. Rumyantsev, and A. Zubrilov, inProperties of Advanced Semiconductor Materials GaN, AlN, InN, BN, SiC, SiGe, edited by M. E. Levinshtein, S. L. Rumyantsev, and M. S. Shur Wiley, *New York*, (2001) , pp. 1–30.
13. Ougazzaden, S. Gautier, T. Moudakir, Z. Djebbour, Z. Lochner, S. Choi, H. J. Kim, J. H. Ryou, R. D. Dupuis, and A. A. Sirenko; Band gap bowing in BGaN thin lms, *Appl. Phys*. Lett, Vol. 93, 083118, aug 25 (2008).
14. Y.Chu , S.Y.Cheng , , M.H.Chiang , Y.J. Liu , C.C. Huang , T.Y. Chen , C.S. Hsu , W.C. Liu , W.Y Cheng , B.C. Lin “Comprehensive study of InGaP/InGaAs/GaAs dual channel pseudomorphic high electron mobility transistors” *Solid-State Electronics* 72 (2012) 22–28.
15. Guenineche and A. Hamdoune “Influence of a BGaN back-barrier on DC and dynamic performances of an AlGaN/GaN HEMT: simulation study “ *Mater. Res. Express* 3 (2016) 055003 .

Figures

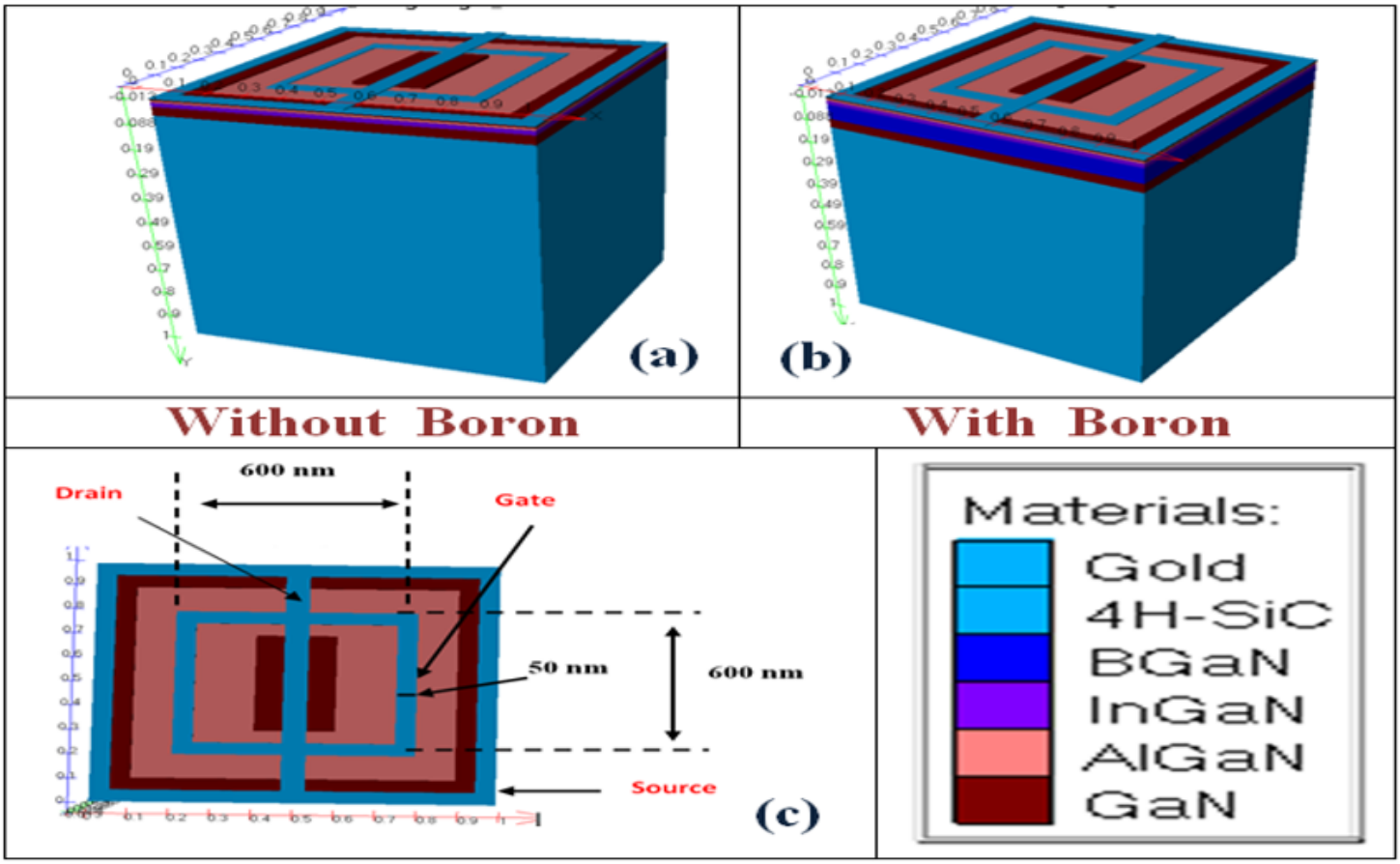

Figure 1

3D view of the AlGaN/InGaN and AlGaN/InGaN/B0.03Ga0.97N HEMTs

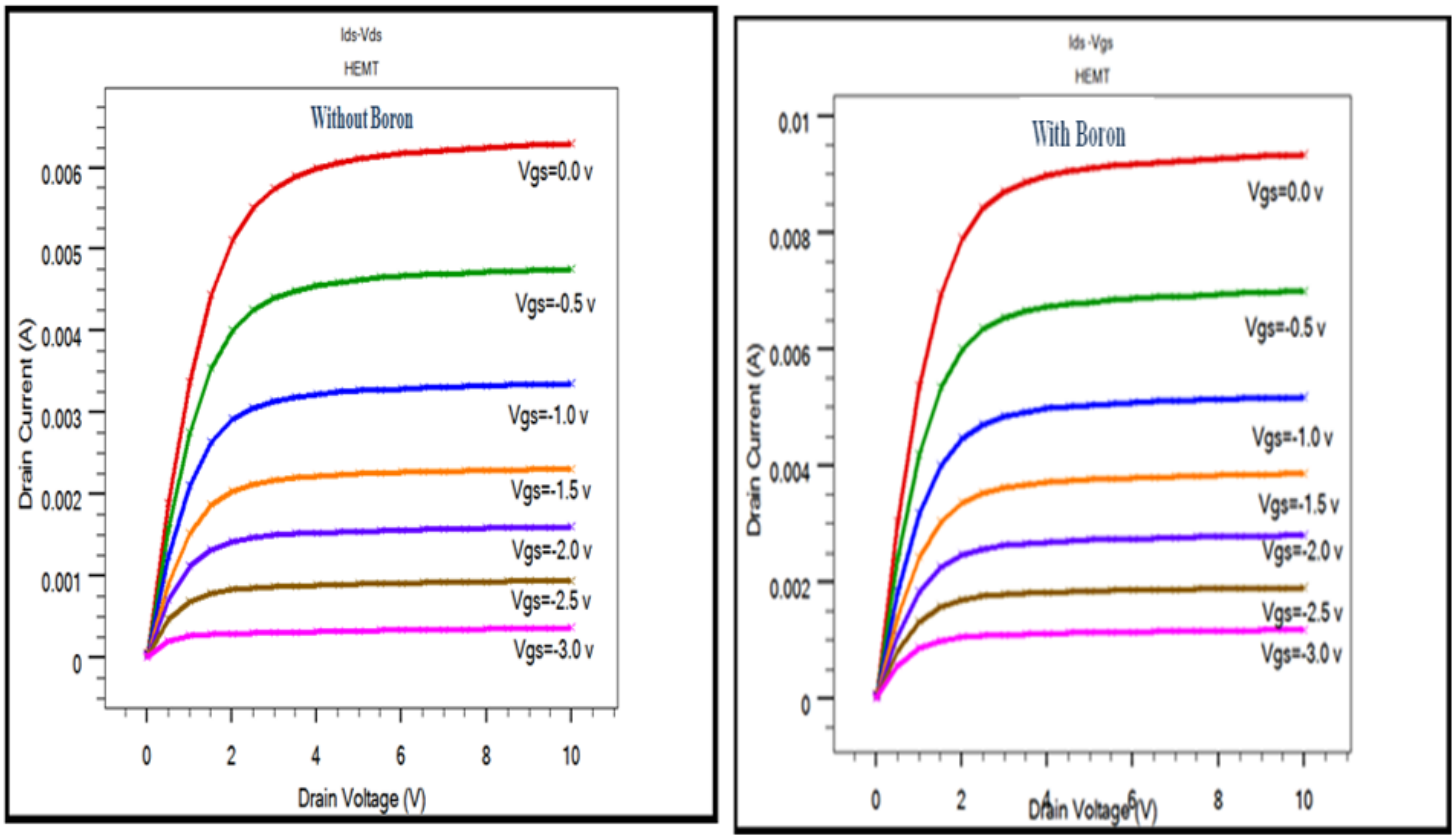

Figure 2

Output characteristic of Al0.1Ga0.9N/In0.2Ga0.8N (a)-HEMT and (b)-HEMTs.

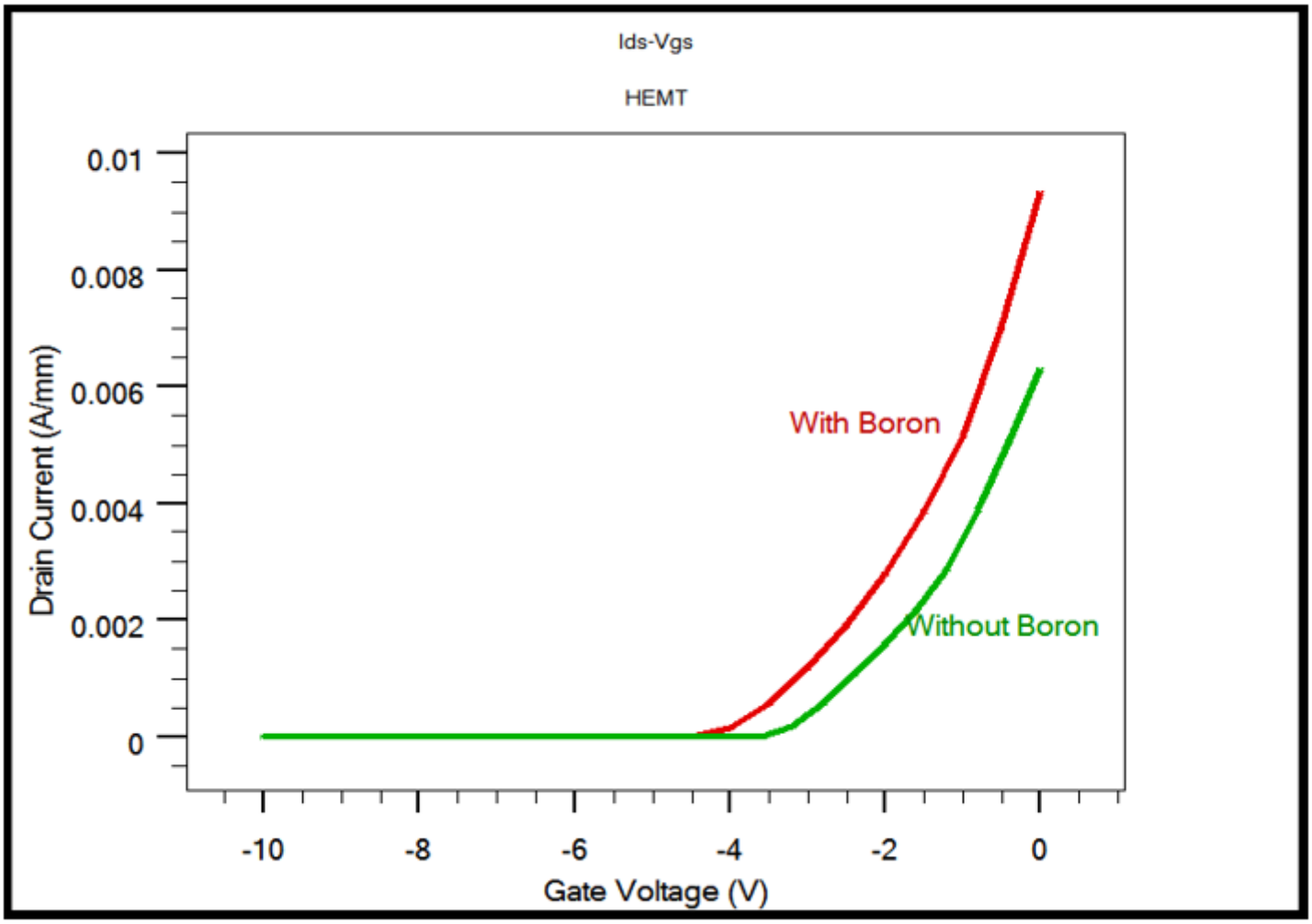

Figure 3

Transfer characteristics of AlGaN/InGaN and AlGaN/InGaN/B0.03Ga0.97N HEMTs.

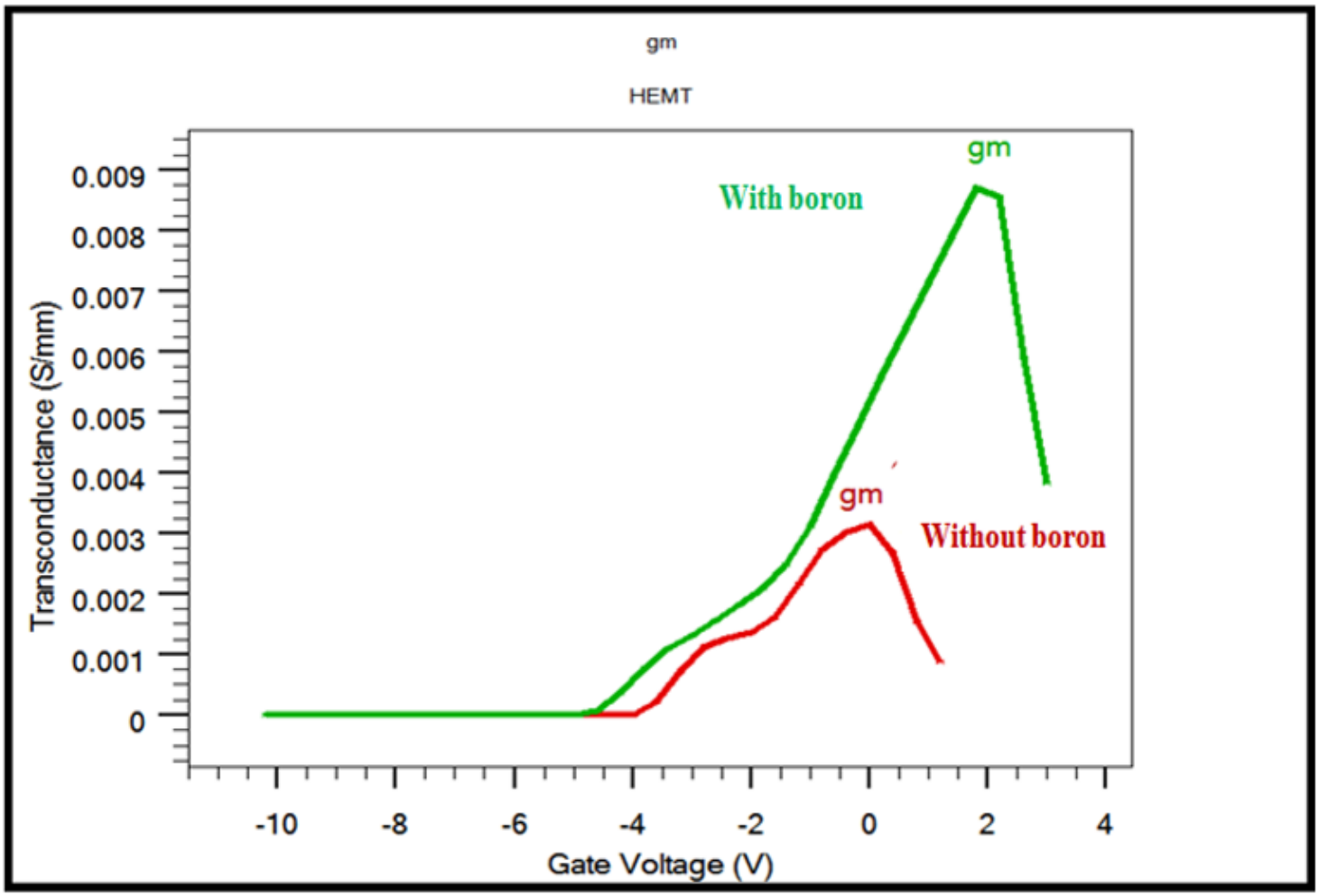

Figure 4

Transconductance of AlGaN/InGaN and AlGaN/InGaN/B0.03Ga0.97N

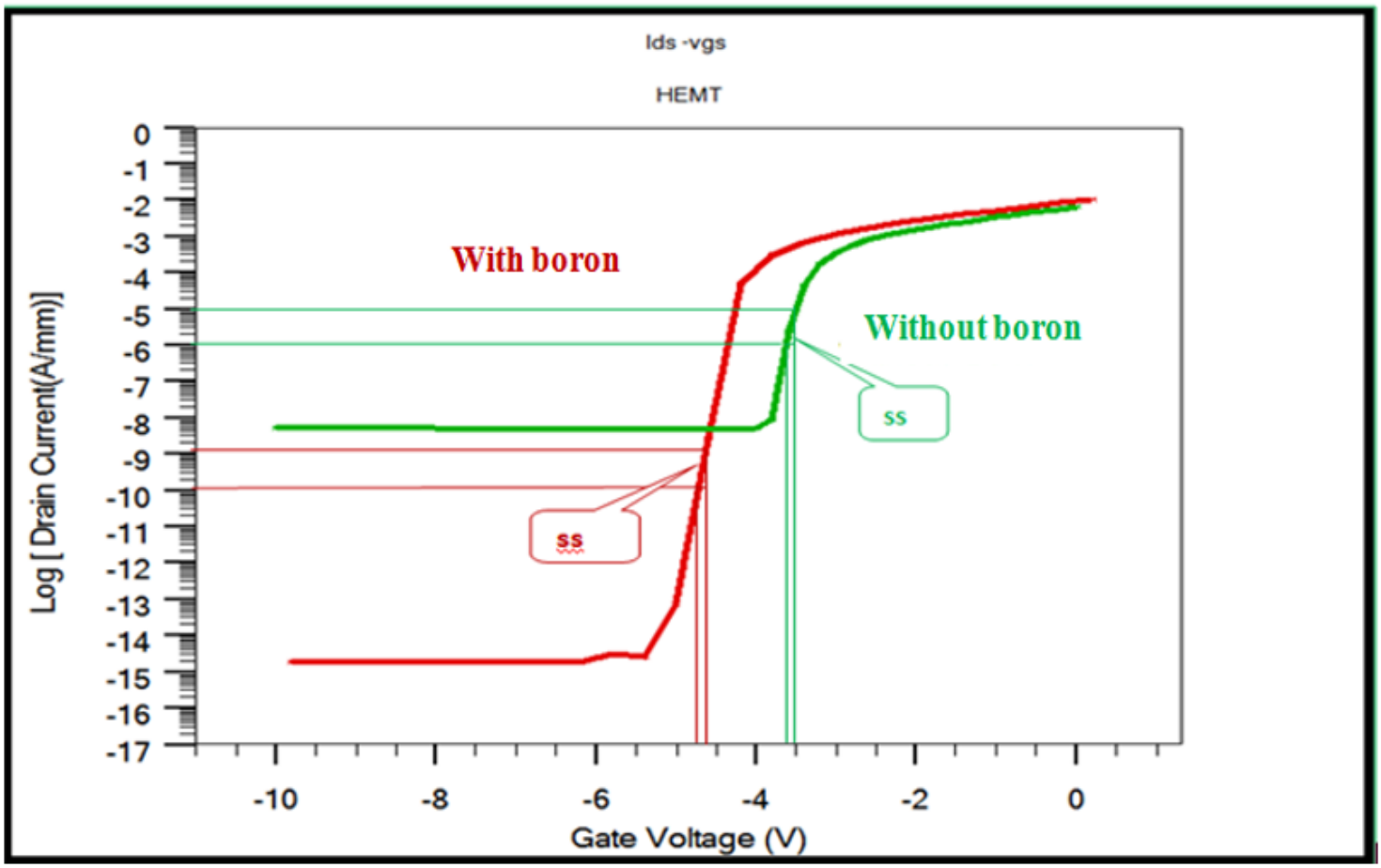

Figure 5

Leakage current of the HEMT AlGaN/InGaN and HEMT AlGaN/InGaN/B0.03Ga0.97N and input characteristic with Vds = 10.0 V.

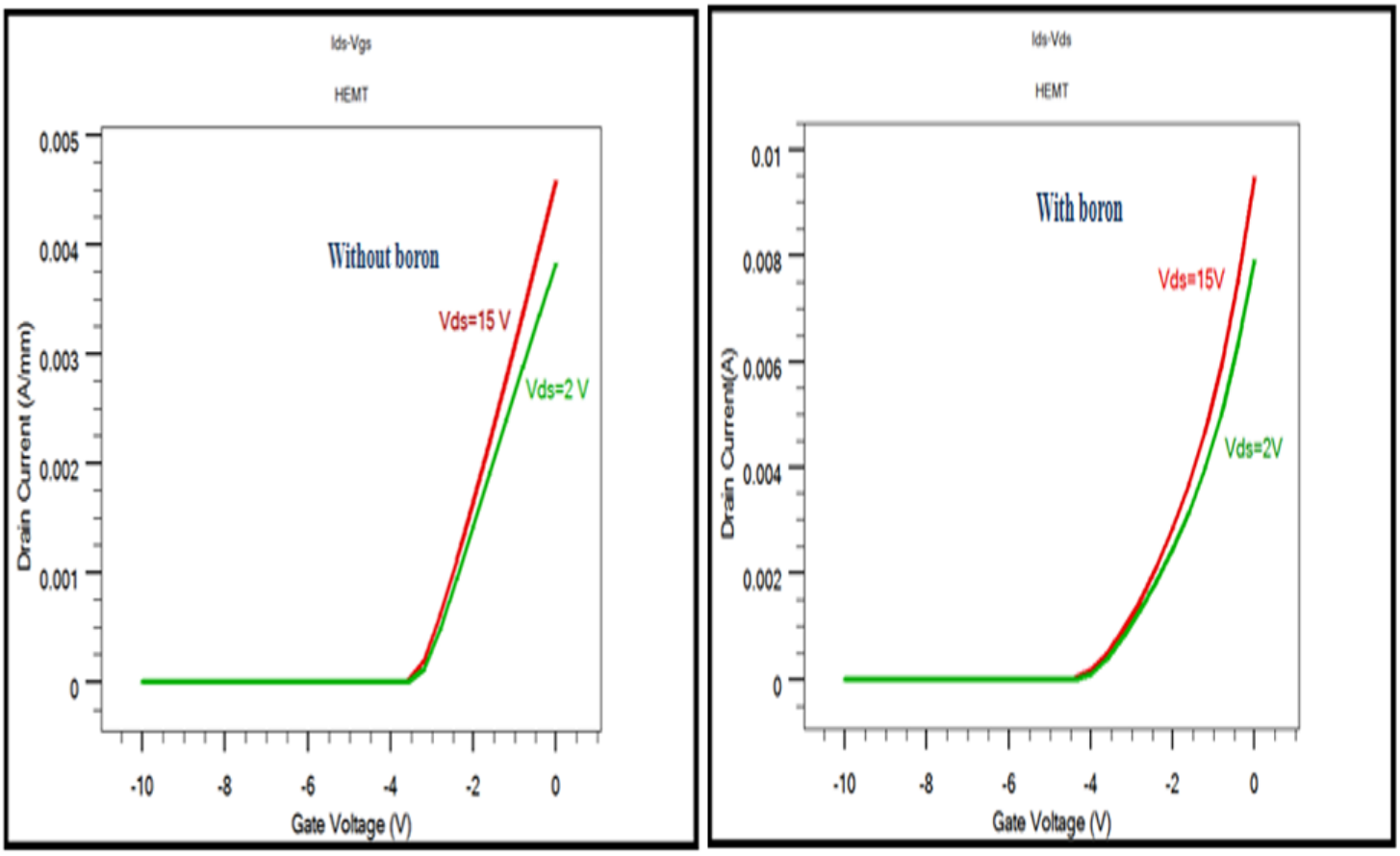

Figure 6

Transfer characteristic of (a)-HEMT and (b)-HEMT for different drain-source voltages (Vds = 2V, Vds = 15 V).

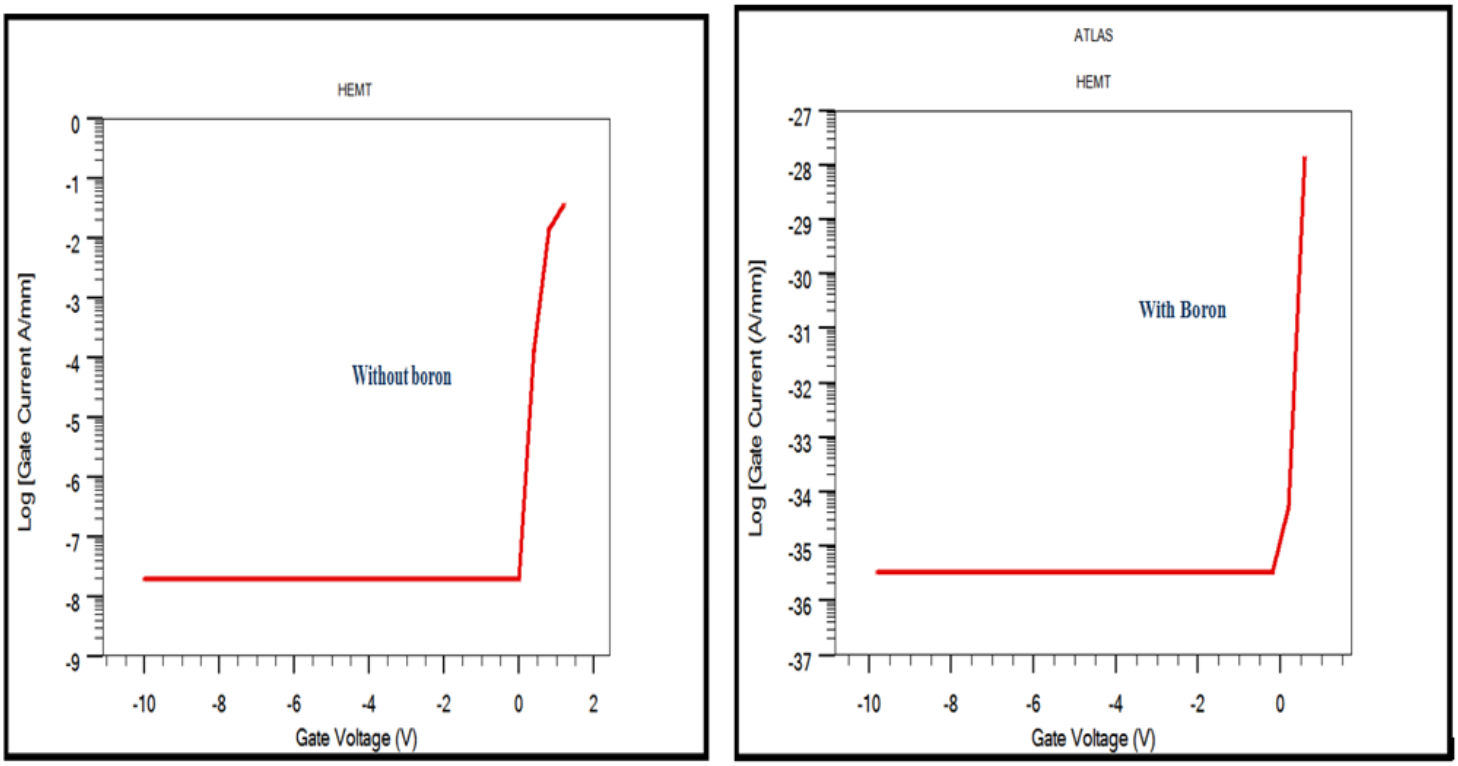

Figure 7

Leakage current of (a)-HEMT and (b)-HEMT for input characteristic with Vds = 10.0 V).

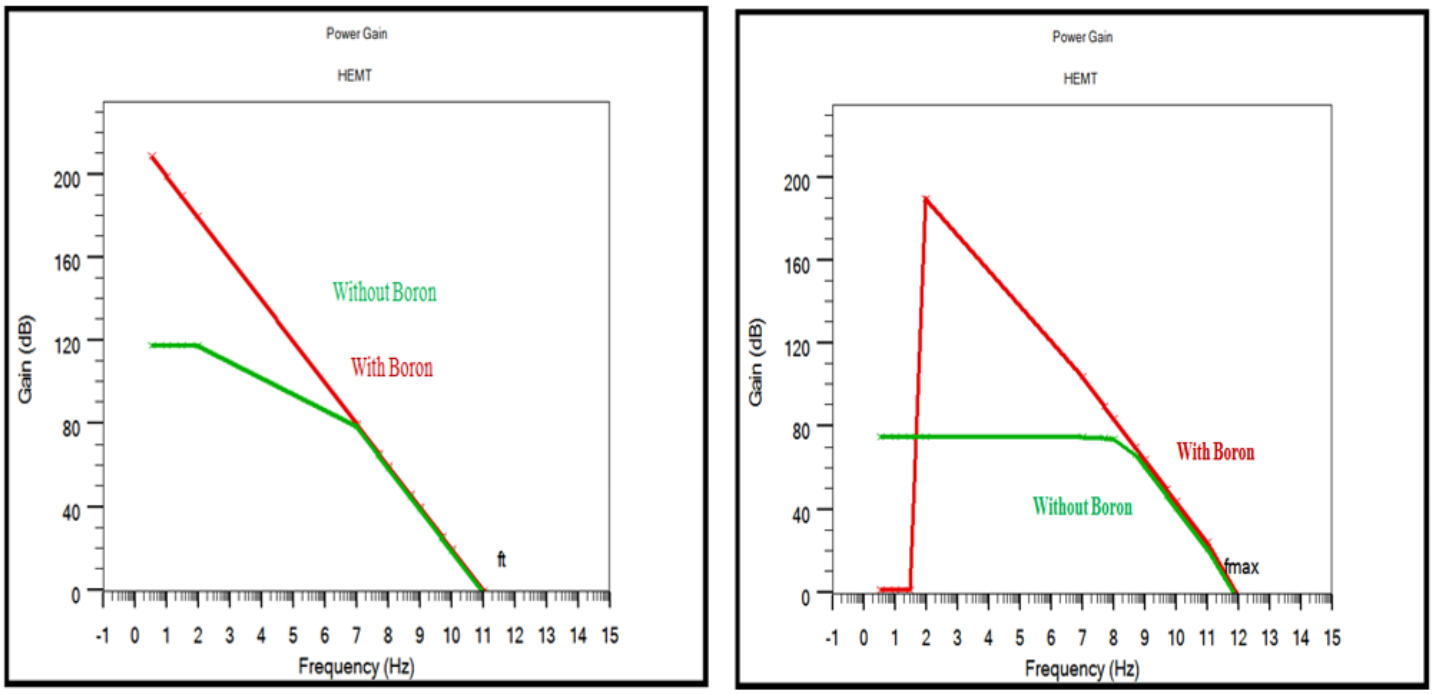

Figure 8

Microwave characteristics ft of the studied a)-HEMT and (b)-HEMT and Microwave characteristics fmax of the studied (a)-HEMT and (b)-HEMT .